

ZnO Nanoparticles: Synthesis and Adsorption Study

K. Prasad¹, Anal K. Jha²

¹University Department of Physics, T.M. Bhagalpur University, Bhagalpur - 812 007, India; *k.prasad65@gmail.com

²University Department of Chemistry, T.M. Bhagalpur University, Bhagalpur - 812 007, India

Received 21 July 2009; revised 27 July 2009; accepted 30 July 2009.

ABSTRACT

A low-cost, green and reproducible probiotic microbe (*Lactobacillus sporogens*) mediated biosynthesis of ZnO nanoparticles is reported. The synthesis is performed akin to room temperature in five replicate samples. X-ray and transmission electron microscopy analyses are performed to ascertain the formation of ZnO nanoparticles. Rietveld analysis to the X-ray data indicated that ZnO nanoparticles have hexagonal unit cell structure. Individual nanoparticles having the size of 5-15 nm are found. A possible involved mechanism for the synthesis of ZnO nanoparticles has been proposed. The H₂S adsorption characteristic of ZnO nanoparticles has also been assayed.

Keywords: ZnO Nanoparticle; Biosynthesis; Nanobiotechnology; Eco-friendly; H₂S Adsorption

1. INTRODUCTION

Nature by dint of its diversity provides exponential possibilities in terms of endearing adaptability of its constituent cohorts. Both bacteria and fungi make such an exciting category of microorganisms having naturally bestowed property of reducing/oxidizing metal ions into metallic/oxide nanoparticles thereby functioning as 'mini' nano-factories. [1,2] It is indeed their chemical constitutions (or metabolic status) which provide them strength to withstand such environmentally diverse habitats. The non-pathogenic, gram positive, mesophilic facultative anaerobe *Lactobacillus*, commonly used for curdling of milk forms part of the beneficial community of microbes present in the human intestinal tract.

Zinc oxide (ZnO) is considered to be a technologically prodigious material having a wide spectrum of applications such as that of a semiconductor ($E_g = 3.37$ eV), magnetic material, electroluminescent material, UV-absorber, piezoelectric sensor and actuator, nanostructure varistor, field emission displaying material, thermoelec-

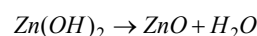
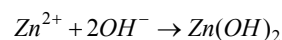
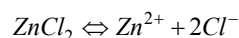
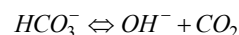
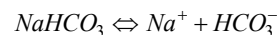
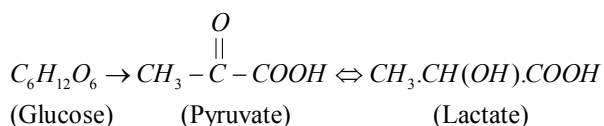
tric material, gas sensor, constituent of cosmetics etc. [3-9] There are several synthesis procedures for the preparation of ultrafine oxide nanoparticles such as sol-gel, hydrothermal, solvothermal, flame combustion, emulsion precipitation, fungus mediated biosynthesis, etc. [10-16] Each method has its own merits and demerits. They are time consuming, capital intensive and require trained manpower. Besides, the development of eco-friendly, 'green' synthesis protocols is in line with the recent RoHS and WEEE legislation stipulated by the EU. Therefore, an urge to develop green synthesis protocols which goes in consonance with the above mentioned stipulations is need of the hour. Microbes exhibit a natural capability to adapt to changes in their environment. Recent research devoted towards the study of interaction between inorganic substances and biological systems has highlighted its potential application for the production of nanomaterials with interesting technological properties. [1,2,17-20] Numerous recent publications have highlighted the potential for microbes, particularly bacteria (including thermophilic) and fungi, to synthesize metallic and/or oxide nanoparticles. [21-35] The facultative nature of *Lactobacilli*, offers the potential to produce nanoparticles under both oxidizing and reducing conditions. [2,18,35]

No work to the best of author's acquaintance has so far been reported regarding the synthesis of ZnO nanoparticles employing *Lactobacilli*. *Lactobacilli* strain, cultured from spores an effort has been taken for synthesizing ZnO nanoparticles (ZnO NPs) in the present work. We have tried to explore a cost effective, green and readily reproducible approach for the purpose of scaling up and subsequent downstream processing. An effort to understand the nano-transformation mechanism of biosynthesis has also been made. It is well established that Hydrogen sulfide (H₂S) is a colorless, corrosive and highly toxic gas, a low concentration of which in air, brings smell of rotten eggs and it substantially contributes towards air pollution. [36,37] The potential of ZnO NPs towards H₂S adsorption has also been assayed in the present study.

2. MATERIALS AND METHODS

2.1. Biosynthesis of ZnO Nanoparticles

Pharmaceutical grade Lactic acid Bacillus spore tablets (SporeLac DS, Sanyko Pharmaceuticals, Japan) were procured and two tablets were dissolved in 50 mL sterile distilled water containing standard carbon and nitrogen source. As per specification, each tablet was capable of producing 120 million spores of the bacterium. The culture solution was allowed to incubate on room temperature overnight. Next day, the presence of *Lactobacillus* was confirmed under an optical microscope. The pH of this source culture solution was observed to be equal to 3. Now, 10 mL of this source culture was doubled in volume by mixing equal volume of sterile distilled water containing nutrients in five different hard glass test tubes. In yet another tube instead of adding the source culture solution, sterile distilled water containing nutrients was pooled and this was treated as control. All these culture tubes were gently heated on a steam bath and were allowed to incubate overnight in laboratory ambience for another 24 hours on orbital shaker. Next day, the pH was taken and found to be in the range of 4-5 in case of culture solution and 7 in case of control. Small quantity of NaHCO₃ was added in culture solution until it attains pH 6. It was brought to this pH as a lower value delays the process of transformation. [2] Similarly, a small volume of distilled water along with carbon and nitrogen source and NaHCO₃ were pipetted in the control tube and the pH = 8.5 were recorded. Analytical reagent grade Zinc Chloride (ZnCl₂) was taken into use for preparing a solution of 0.25(M) strength at room temperature. Control solution was prepared by adding 100 mL sterile distilled water, carbon and nitrogen containing nutrients and the mild base in known quantitative ratio (5:1:1). To each of these tubes, 20 mL of Zinc Chloride solution was added. The pH of the control tube was noted to be 8-9 in 5 different set of experiments. Culture solution containing tubes including control tube were heated on the steam bath up to 80°C for 5 to 10 minutes. An appearance of starch like haziness in solution and white deposition at the bottom of the tube was perceived as an indication of commencement of transformation. No such deposition or haziness was observed in control tube. The tubes were allowed to incubate in the laboratory ambience for another 9 hours, after which distinctly markable coalescent white clusters deposited at the bottom of all the tubes except in control. A remarkable change in pH was observed at this stage (6.0 to 7.5) excluding control (8 to 9). The chemical reactions which proceed in the culture medium may be as follows:



2.2. Characterization

The formation of ZnO NPs was checked by X-ray diffraction (XRD) technique using an X-ray diffractometer (XPRT-PRO, Pan Analytical) with CuK_α radiation ($\lambda = 1.5406\text{\AA}$) over a wide range of Bragg angles ($10^\circ \leq 2\theta \leq 80^\circ$). The XY (2θ vs. intensity) data obtained from this experiment were plotted with the WinPLOT program and the angular positions of the peaks were obtained with the same program. [38] The dimensions of the unit cell, hkl values and space group of ZnO NPs were obtained using the DICVOL program in the FullProf 2000 software package and then refinement was carried out through the profile matching routine of FullProf. [39] The Bragg peaks were modeled with pseudo-Voigt function and the background was estimated by linear interpolation between selected background points. The crystallite size (D) and the lattice strain of ZnO NPs were estimated by analyzing the broadening of X-ray diffraction peaks, using Williamson-Hall approach. [40]

$$\eta \cos \theta = (K\lambda / D) + 2(\Delta\xi / \xi) \sin \theta \quad (1)$$

where η is diffraction peak width at half intensity (FWHM) and $\Delta\xi / \xi$ is the lattice strain and K is the Scherrer constant (0.89). The term $K\lambda/D$ represents the Scherrer particle size distribution. TEM micrograph of ZnO NPs was obtained using Hitachi H-7500 transmission electron microscope. The specimen was suspended in distilled water, dispersed ultrasonically to separate individual particles, and two drops of the suspension deposited onto holey-carbon coated copper grids.

3. RESULTS

3.1. Structural and Microstructural Studies

Rietveld refinements on the X-ray (XRD) data were done on ZnO NPs, selecting the space group $P6/mmm$. **Figure 1** depicts the observed, calculated and difference XRD profiles for ZnO NPs after final cycle of refinement. It can be seen that the profiles for observed and calculated one are perfectly matching. The value of χ^2 comes out to be equal to 3.16, which may be considered to be very good for estimations. The profile fitting procedure adopted was minimizing the χ^2 function. [41] The XRD analyses indicated that ZnO NPs has a hexagonal unit cell. The crystal data and refinement factors of ZnO

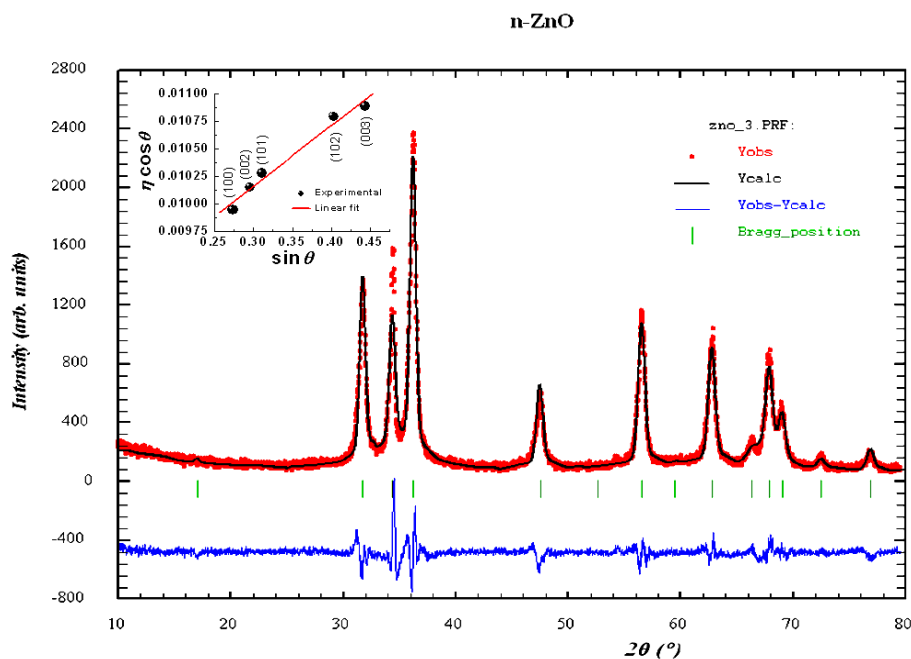


Figure 1. Rietveld refined pattern of ZnO NPs in the space group $P6/mmm$. Symbols represent the observed data points and the solid lines their Rietveld fit. Inset: Williamson-Hall plot for ZnO NPs.

Table 1. The crystal data and refinement factors of ZnO NPs obtained from X-ray powder diffraction data.

Parameters	Results	Description of parameters
Crystal System	Hexagonal	R_p (profile factor) = $100[\sum y_i - y_{ic} / \sum y_i]$, where y_i is the observed intensity and y_{ic} is the
Space group	$P6/mmm$	calculated intensity at the i^{th} step.
a (Å)	3.2524	R_{wp} (weighted profile factor) = $100[\sum \omega_i y_i - y_{ic} ^2 / \sum \omega_i (y_i)^2]^{1/2}$, where $\omega_i = 1/\sigma_i^2$ and σ_i^2
b (Å)	3.2524	is variance of the observation.
c (Å)	5.2120	R_{exp} (expected weighted profile factor) = $100[(n-p)/\sum \omega_i (y_i)^2]^{1/2}$, where n and p are the
α (°)	90.000	number of profile points and refined parameters, respectively.
β (°)	90.000	R_B (Bragg factor) = $100[\sum I_{obs} - I_{calc} / \sum I_{obs}]$, where I_{obs} is the observed integrated intensity and I_{calc} is the calculated integrated intensity.
γ (°)	120.000	R_F (crystallographic R_F factor) = $100[\sum F_{obs} - F_{calc} / \sum F_{obs}]$, where F is the structure
V (Å ³)	47.7463	factor, $F = \sqrt{I/L}$, where L is Lorentz polarization factor.
R_p	25.2	$\chi^2 = \sum \omega_i (y_i - y_{ic})^2$.
R_{wp}	23.8	d (Durbin-Watson statistics) = $\sum \{[\omega_i (y_i - y_{ic}) - \omega_{i-1} (y_{i-1} - y_{i-1})]^2\} / \sum [\omega_i (y_i - y_{ic})]^2$.
R_{exp}	13.4	$Q_D = \text{expected } d$.
R_B	0.175E-3	S (goodness of fit) = (R_{wp}/R_{exp}) .
R_F	0.133E-3	
χ^2	3.16	
d	0.6844	
Q_D	1.9059	
S	1.776	

NPs obtained from XRD data are depicted in **Table 1**. The lattice parameter as obtained for ZnO NPs is in good agreement with the literature report (PCPDF No. #89-0510). Inset **Figure 1** illustrates the Williamson-Hall plot for ZnO NPs. A linear least square fitting

to $\eta \cos\theta - \sin\theta$ data yielded the values of average crystallite size and lattice strain respectively to be 11 nm and 0.0035. The low value of lattice strain might be due to the fact that the procedure adopted in the synthesis of nanoparticles is natural (biosynthetic) one.

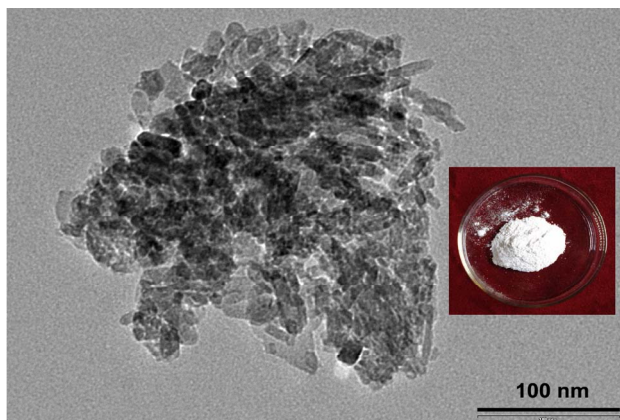


Figure 2. TEM photograph of ZnO NPs. Inset: ZnO NPs.

Figure 2 shows the TEM micrograph of ZnO NPs (inset **Figure 2**) being formed using *Lactobacillus* strain. The micrograph clearly illustrates the nanoparticles with tubules and other irregular forms having the sizes of 5-15 nm. The measurement of size was carried along the diameter of the particles. The difference in particle size is possibly due to the fact that the nanoparticles are being formed at different times. It is found that the size of the ZnO NPs estimated using TEM analysis to be in fairly good agreement with the size estimated by the Williamson-Hall approach.

3.2. Adsorption Study

Figure 3 shows the experimental setup to assess the adsorption capacity of synthesized ZnO NPs as well as bulk ZnO. Freshly prepared H₂S was allowed to pass through the equal quantities of bulk ZnO and ZnO NPs (5 gm each) for a fixed span of time (30 min.) and flow of gas was suitably regulated. The degree of absorption was assessed directly through the change in colour of lead acetate solution (from clear solution to black). It was observed that the presence of bulk ZnO blackens the

solution (due to formation of lead sulfide) within 5 minutes, while ZnO NPs does the same in 25 min. The experiment was pursued as five replicates and each gave approximately the same result. This happens due to the fact that nanoparticles have large surface to volume ratio and hence a high surface activity and these features might have led to better degree of adsorption of H₂S in comparison to its bulk counterpart. H₂S absorption by ZnO proceeds according to the reaction: $\text{ZnO} + \text{H}_2\text{S} \rightarrow \text{ZnS} + \text{H}_2\text{O}$ that results into formation of inert Zinc sulfide.

4. DISCUSSION

Lactobacilli cells are prokaryotes in terms of cellular organization. They are gram positive (a thick peptidoglycan cell wall) bacteria showing facultative anaerobic properties, which probably make them suitable candidate microorganism for biosynthesis of metal as well as oxide nanoparticle. Like most of the bacteria, they have a negative electro-kinetic potential; which readily attracts the cations and this step probably acts as a trigger of the procedure of biosynthesis. Earlier, such a possibility of biosorption and bioreduction had been reported in case of silver iodide by the *Lactobacillus* sp. A09*. [42] The mesophilic, non-pathogenic and facultatively anaerobic microbe like *Lactobacillus* has robust metabolic capabilities. Addition of simple carbohydrates into the culture medium tends to lower the value of oxidation-reduction potential (or the Eh value). The oxidation-reduction potential expresses the quantitative character of degree of aerobiosis having a designated unit expressed as rH₂ (the negative logarithm of the partial pressure of gaseous hydrogen). By controlling rH₂ of the nutrient medium, conditions can be engineered for the growth of anaerobes in the presence of oxygen by lowering the rH₂ and also by cultivating the aerobes in anaerobic conditions by increasing the rH₂ of the medium.

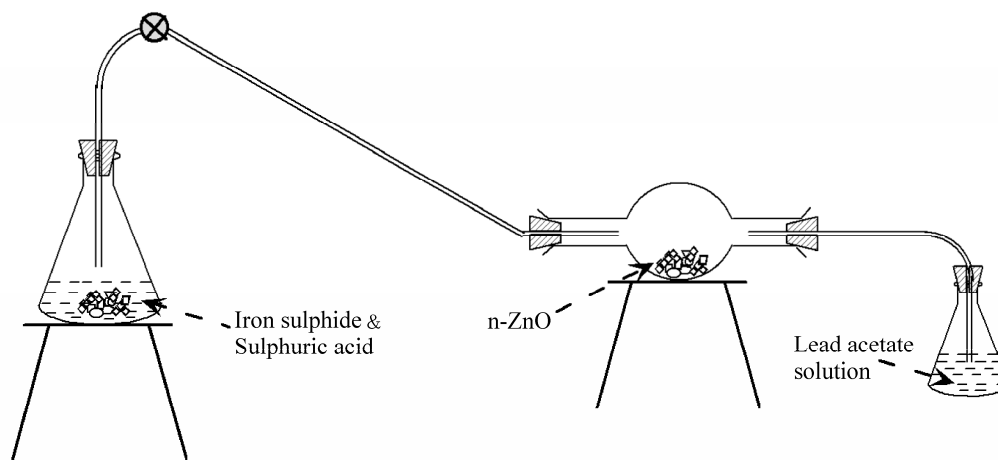


Figure 3. Experimental set up to study adsorption of H₂S by ZnO NPs.

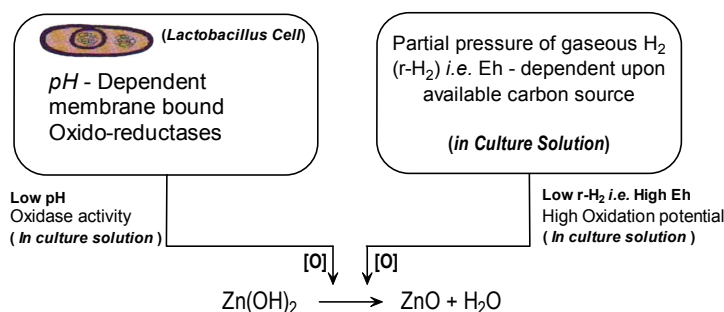


Figure 4. Schematic showing the mechanism for the biosynthesis of ZnO NPs.

Composition of nutrient media, therefore; plays a pivotal role in biosynthesis of metallic and/or oxide nanoparticles which is done in the present investigation. Energy yielding material – suitable carbohydrate (which controls the value of $r\text{H}_2$), the ionic status of the medium pH and overall oxidation-reduction potential (Eh) of the culture medium, all these factors cumulatively negotiate the synthesis of ZnO nanoparticles in the presence of *Lactobacillus* strain. Taking use of the above mentioned facts, our group had earlier reported synthesis of metallic cadmium [18], silver [17,34,43] as well as antimony oxide [1,44] and titanium dioxide. [2] A mildly acidic pH also activates the membrane bound oxidoreductases and makes the requisite ambience for an oxide nanoparticle synthesis as illustrated in **Figure 4**. Therefore, compared to other techniques, the present procedure is less expensive more reproducible, emphatically non-toxic and a truly green approach.

A large quantity of hydrogen sulfide is liberated in gas and petroleum industries and has been considered as a major pollutant. Besides, according to the international environmental regulations, H_2S contained in the acid gases should be effectively removed before its release to atmosphere. Its characteristic odor could easily be perceived in a dilution of 0.002 mg/L in ambient air. Intake of higher concentrations, could lead to the collapse from respiratory failure. For the purpose of protection, the concentration should be reduced to less than 15 ppm. [45] Pollution of underground aquifers has been a prevalent problem in the areas adjoining oil and gas reserves, which miserably affects the health of nearby inhabitants. Use of ZnO NPs produced using present green and low cost protocol based devices could prove to be an effective step towards mitigation of the menace.

5. CONCLUSIONS

The present biosynthesis method is a green low cost approach, capable of producing ZnO NPs nearby room temperature. The synthesis of ZnO NPs might have resulted due to variation in the level of $r\text{H}_2$ or pH, which activates the pH sensitive oxido-reductases. ZnO

nanoparticles could be effective in controlling the pollution generated due to H_2S in air as well as underground aquifers. However, bright possibility exists with regard to the development of different products/devices in order to get rid of the menace of different forms of air and/or water pollution such as face masks, water filters, de-odorizing cakes and screens. Cosmetic industries can bank upon this product in order to synthesize sunscreen lotions etc., which would be done in the immediate future.

REFERENCES

- [1] Jha, A.K., Prasad, K. and Prasad, K. (2009) A green low-cost biosynthesis of Sb_2O_3 nanoparticles. *Biochem Engg J*, **43**, 303-306.
- [2] Jha, A.K., Prasad, K. and Kulkarni, A.R. (2009) Synthesis of TiO_2 nanoparticles using microorganisms. *Colloid Surf B: Bioint*, **71**, 226–229.
- [3] Park, S., Lee, J.-H., Kim, H.-S., Park, H.-J. and Lee, J. C. (2009) Effects of ZnO nanopowder dispersion on photocatalytic reactions for the removal of Ag^+ ions from aqueous solution. *J Electroceram*, **22**, 105–109.
- [4] Wang, Z.L. (2008) Energy harvesting for self-powered nanosystems. *Nano Res*, **1**, 1-8.
- [5] Botello-Méndez, A.R., López-Urías, F., Terrones, M. and Terrones, H. (2008) Enhanced ferromagnetism in ZnO nanoribbons and clusters passivated with sulfur. *Nano Res*, **1**, 420-426.
- [6] Grigorjeva, L., Millers, D., Grabis, J., Monty, C., Kalinko, A., Smits, K., Pankratov, V. and Lojkowski, W. (2008) Luminescence properties of ZnO nanocrystals and ceramics. *IEEE Trans Nucl Sci*, **55**, 1551-1555.
- [7] Daneshvar, N., Aber, S., Seyed Dorraji, M.S., Khataee, A.R. and Rasoulifard, M.H. (2008) Preparation and investigation of photocatalytic properties of ZnO nanocrystals: effect of operational parameters and kinetic study. *Int J Chem Biomol Engg*, **1**, 24-29.
- [8] Lee, C.-Y., Haung, Y.-T., Su, W.-F. and Lin, C.-F. (2006) Electroluminescence from ZnO nanoparticles/organic nanocomposites. *Appl Phys Lett*, **89**, 231116-231118.
- [9] Tong, Y.H., Liu, Y.C., Lu, S.X., Dong, L., Chen, S.J. and Xiao, Z.Y. (2004) The optical properties of ZnO nanoparticles capped with polyvinyl butyral. *J Sol-Gel Sci Tech*, **30**, 157-61.

- [10] Moghaddam, A.B., Nazari, T., Badraghi, J. and Kazemzad, M. (2009) Synthesis of ZnO nanoparticles and electrodeposition of polypyrrole/ZnO nanocomposite film. *Int J Electrochem Sci*, **4**, 247–257.
- [11] Shokuhfar, T., Vaezi, M.R., Sadrnezhad, S.K. and Shokuhfar, A. (2008) Synthesis of zinc oxide nanopowder and nanolayer via chemical processing. *Int J Nanomanufacturing*, **2**, 149-162.
- [12] Kim, S.-J. and Park, D.-W. (2007) Synthesis of ZnO nanopowder by thermal plasma and characterization of photocatalytic property. *Appl Chem*, **11**, 377-380.
- [13] Vaezi, M.R. and Sadrnezhad, S. (2007) Nanopowder synthesis of zinc oxide via solochemical processing. *Material Design*, **28**, 515–519.
- [14] Ge, M.Y., Wu, H.P., Niu, L., Liu, J.F., Chen, S.Y., Shen, P.Y., Zeng, Y.W., Wang, Y.W., Zhang, G.Q. and Jiang, J.Z. (2007) Nanostructured ZnO: from monodisperse nanoparticles to nanorods. *J Cryst Growth*, **305**, 162–166.
- [15] Hambrock, J., Rabe, S., Merz, K., Birkner, A., Wohlfart, A., Fischer, R.A. and Driess, M. (2003) Low-temperature approach to high surface ZnO nanopowders and a non-aqueous synthesis of ZnO colloids using the single-source precursor $[\text{MeZnOSiMe}_3]_4$ and related zinc siloxides. *J Mater Chem*, **13**, 1731–1736.
- [16] Kwon, Y.J., Kim, K.H., Lim, C.S. and Shim, K.B. (2002) Characterization of ZnO nanopowders synthesized by the polymerized complex method via an organochemical route. *J Ceram Process Res*, **3**, 146-149.
- [17] Prasad, K., Jha, A.K. and Kulkarni, A.R. (2008) Yeast mediated synthesis of silver nanoparticles. *Int J Nanosci Nanotech*, in press.
- [18] Prasad, K., Jha, A.K. and Kulkarni, A.R. (2007) Microbe mediated nano transformation: cadmium. *NANO: Brief Rep Rev*, **2**, 239-242.
- [19] Shahverdi, A.R., Minaeian, S., Shahverdi, H.R., Jamalifar, H. and Nohi, A.-A. (2007) Rapid synthesis of silver nanoparticles using culture supernatants of enterobacteria: a novel biological approach. *Process Biochem*, **42**, 919-923.
- [20] Husseiny, M.I., Abd El-Aziz, M., Badr, Y. and Mahmoud, M.A. (2007) Biosynthesis of gold nanoparticles using *Pseudomonas aeruginosa*. *Spectrochim Acta Part A*, **67**, 1003-1006.
- [21] Klaus, T., Joerger, R., Olsson, E. and Granqvist, C.G. (2001) Bacteria as workers in the living factory: metal accumulating bacteria and their potential for materials science. *Trends Biotechnol*, **19**, 15-20.
- [22] Gericke, M. and Pinches, A. (2006) Biological synthesis of metal nanoparticles. *Hydrometallurgy*, **83**, 132-140.
- [23] Senapati, S., Ahmad, A., Khan, M.I., Sastry, M. and Kumar, R. (2005) Extracellular biosynthesis of bimetallic Au-Ag alloy nanoparticles. *Small*, **1**, 517-520.
- [24] Vigneshwaran, N., Ashtaputre, N.M., Varadarajan, P.V., Nachane, R.P., Paralizar, K.M. and Balasubramanya, R.H. (2007) Biological synthesis of silver nanoparticles using the fungus *Aspergillus flavus*. *Mater Lett*, **61**, 1413-1418.
- [25] Mohanpuria, P., Rana, N.K. and Yadav, S.K. (2008) Biosynthesis of nanoparticles: technological concepts and future applications. *J Nanopart Res*, **10**, 507-517.
- [26] Mandal, D., Bolander, M.E., Mukhopadhyay, D., Sarkar, G. and Mukherjee, P. (2006) The use of microorganisms for the formation of metal nanoparticles and their application. *Appl Microbiol Biotechnol*, **69**, 485-492.
- [27] Bansal, V., Rautaray, D., Barred, A., Ahire, K., Sanyal, A. and Ahmad, A. (2005) Fungus-mediated biosynthesis of silica and titania particles. *J Mater Chem*, **15**, 2583-2589.
- [28] Sadowski, Z., Maliszewska, I.H., Grochowalska, B., Polowczyk, I. and Koźlecki, T. (2008) Synthesis of silver nanoparticles using microorganisms. *Mater Sci-Poland*, **26**, 419-424.
- [29] Joerger, R., Klaus, T. and Granqvist, C.G. (2001) Biologically produced silver-carbon composite materials for optically functional thin-film coating. *Adv Mater*, **12**, 407-409.
- [30] Mukherjee, P., Ahmad, A., Mandal, D., Senapati, S., Sainkar, S.R., Khan, M.I., Parischa, R., Ajaykumar, P.V., Alam, M., Kumar, R. and Sastry, M. (2001) Fungus-mediated synthesis of silver nanoparticles and their immobilization in the mycelial matrix: A novel biological approach to nanoparticle synthesis. *Nano Lett*, **1**, 515-519.
- [31] Ankamwar, B., Damle, C., Absar, A. and Sastry, M. (2005) Biosynthesis of gold and silver nanoparticles using *Emblica Officinalis* fruit extract, their phase transfer and trans-metallation in an organic solution. *J Nanosci Nanotechnol*, **10**, 1665-1671.
- [32] Armendariz, V., Herrera, I., Peralta-Videa, J.R., Jose-Yacaman, M., Toroiani, H., Santiago, P. and Gardea-Torresdey, J.L. (2004) Size controlled gold nanoparticles formation by *Avena sativa* biomass: use of plants in nanobiotechnology. *J Nanopart Res*, **6**, 377-382.
- [33] Shankar, S.S., Rai, A., Ahmad, A. and Sastry, M. (2004) Rapid synthesis of Au, Ag and bimetallic Au core-Ag shell nanoparticles using Neem (*Azadirachta indica*) leaf broth. *J Colloid Interface Sci*, **275**, 496-502.
- [34] Jha, A. K., Prasad, K., Kumar, V. and Prasad, K. (2009) Biosynthesis of silver nanoparticles using *Eclipta* leaf. *Biotechnol Prog*, in print.
- [35] Nair, B. and Pradeep, T. (2002) Coalescence of nanoclusters and formation of submicron crystallites assisted by *Lactobacillus* strains. *Cryst Growth Design*, **2**, 293-298.
- [36] Haimour, N., El-Bishtawi, R. and Ail-Wahbi, A. (2005) Equilibrium adsorption of hydrogen sulfide onto CuO and ZnO. *Desalination*, **181**, 145-152.
- [37] Duan, Z., Sun, R., Liu, R. and Zhu, C. (2007) Accurate thermodynamic model for the calculation of H₂S solubility in pure water and brines. *Energ Fuel*, **21**, 2056-2065.
- [38] Roisnel, J. and Rodriguez-Carvajal, J. (2000) WinPLOTR; laboratoire leon brillouin (CEA-CNRS) centre d'Etudes de saclay: gif sur yvette cedex. France.
- [39] Rodriguez-Carvajal, J. (2000) FullProf: A Rietveld Refinement and Pattern Matching Analysis Program, (Version: April 2008). *Laboratoire Léon Brillouin (CEA-CNRS)*, France.
- [40] Williamson, G.K. and Hall, W.H. (1953) X-ray line broadening from filed aluminum and wolfram. *Acta Metall*, **1**, 22-31.
- [41] McCusker, L. B., Von Dreele, R. B., Cox, D. E., Louër, D. and Scardi, P. (1999) Rietveld refinement guidelines. *J Appl Cryst*, **32**, 36-50.
- [42] Fu, J.K., Liu, Y.Y., Gu, P.Y., Tang, D.L., Lin, Z.Y., Yao, B.X. and Wen, S.Z. (2000) Spectroscopic characterization on the biosorption and bioreduction of Ag(I) by

- Lactobacillus* sp A09* . *Acta Physico-Chimica Sinica*, **16**, 779-782.
- [43] Jha, A.K., Prasad, K., Prasad, K. and Kulkarni, A.R. (2009) Plant system: nature's nanofactory. *Colloid Surf B: Bioint*, **73**, 219-223.
- [44] Jha, A.K., Prasad, K. and Prasad, K. (2009) Biosynthesis of Sb₂O₃ nanoparticles: A low cost green approach. *Bio-technol J*, in press.
- [45] Davidson, E. (2004) Method and composition for scavenging sulphide in drilling fluids. US Patent: 6476611.